Spatial anisotropy of velocity fluctuations on small length scales in a Taylor-Couette cell

Knut Jørgen Måløy* and Walter Goldburg
Department of Physics and Astronomy, University of Pittsburgh, Pittsburgh, Pennsylvania 15260
(Received 16 November 1992)

Homodyne light scattering was used to measure a component of the velocity difference $\delta v(\ell)$ on small length scales ℓ in a vertical Taylor-Couette cell with a rotating inner cylinder. In addition, large-scale flow patterns were recorded photographically. Both types of measurements revealed the presence of rolls, out to very large Reynolds number R. The small-scale measurements of the mean value of $\delta v(\ell)$ exhibit a periodicity that appears near the onset of chaos. Various scaling properties of the flow were investigated.

PACS number(s): 47.27.Cn

INTRODUCTION

Fluid flow in a Taylor-Couette cell with the inner cylinder rotating and the other cylinder fixed, will go through several transitions before it becomes turbulent [1]. The large-scale features of the flow are studied by adding Kalliroscopic flakes to the fluid. These small platelets are aligned by the local shear, producing patterns that are readily photographed. Another widely used method for probing the local velocity field is laser Doppler velocimetry (LDV), which measures the time dependence of $v(t)$, the streamwise velocity component at a point. Here we describe experiments using a third method, photon homodyne correlation spectroscopy, or HCS. Like LDV it requires the seeding of the fluid with small particles that scatter light. But rather than recording the velocity versus time, HCS measures, at an arbitrarily chosen point, a time average $\langle \delta v(\ell) \rangle$ of a component $\delta v(\ell)$ of the instantaneous velocity *difference* $\delta \mathbf{v}(\ell)$ between two closely spaced points separated by a distance ℓ. Here the velocity component $\delta v(\ell)$ is the projection of $\delta \mathbf{v}(\ell)$ in the direction of the momentum transfer vector $\mathbf{q}$ of the scattered light.

This experiment compares small-scale velocity differences with the large-scale roll structure and modulations of it that are visible to the eye. We will concentrate on the variation of $\langle \delta v(\ell, y) \rangle$ with vertical position (y) in the cell. In most of our experiments ℓ is 0.2 mm, which is much smaller than the spacing between the rolls that appear when the Reynolds number R exceeds a critical value, $R_c = 125$. Here R is defined as $R = Vd/\nu$, where d is the gap distance between the inner and the outer cylinder, V the rotation speed of the inner cylinder, and ν the kinematic viscosity. Unless stated otherwise, it will be assumed that ℓ has the value $\ell = 0.2$ mm, and we will use the simplified notation $\langle \delta v(y) \rangle \equiv \langle \delta v(\ell = 0.2 \text{ mm}, y) \rangle$. Our principal findings are now summarized.

Even when R/R_c is only slightly greater than unity, $\langle \delta v(y) \rangle$, on a scale $\ell = 0.2$ mm, is periodic in y and has the same wavelength as the wavy vortex flow seen in Fig. 1. However, when R reaches the value at which the velocity becomes chaotic ($R/R_c \simeq 11$), $\langle \delta v(y) \rangle$ develops new maxima, as may be seen in Fig. 2 when $R/R_c = 11.4$. The spacing of these new maxima is the same as the roll spacing. This secondary periodicity, as well as primary oscillations, persist to $R/R_c = 91.3$. This may be seen in Fig. 2, where $\langle \delta v(y) \rangle$ is plotted (in dimensionless units defined below) as a function of height y in the cell. It has long been known that a large-scale roll structure exists in Couette flow out to R/R_c as large as 1600 [2]. The present measurements establish that this periodicty exists at small scales as well. In fact, the amplitude of these oscillations in $\langle \delta v(y) \rangle$, normalized by the height-averaged mean value, shows no decrease with increasing R, even when the system is in the turbulent vortex flow regime ($R/R_c > 22$). In this regime the power spectrum $S(\omega)$ of the local velocity $v(t)$ has no sharp frequency components, but rather is broad banded [3, 4].

An initial motivation for this experiment was the expectation that at sufficiently large values of R and sufficiently small ℓ, the flow would become turbulent in the Kolmogorov sense. According to this model of fully developed turbulence [5], $\langle \delta v(\ell) \rangle$ is proportional to ℓ^{ζ}, with $\zeta = 1/3$ in the inertial range. The smallest eddy size for which this type of scaling is expected to hold is the dissipative scale, η, which decreases as R is increased [6]. In a Couette cell with a much smaller aspect ratio than the one used here, this type of scaling was indeed observed [7], with R/R_c of the order of 1000 and ℓ in the range 0.2 to 1.2 mm. The geometry of that cell was very different from the one used here. In that work no attempt was made to probe the variation of $\langle \delta v(\ell, y) \rangle$ as a function of the vertical position of observation y. In the cell used here the ℓ dependence of $\langle \delta v(\ell, y) \rangle$ was also studied. Power-law behavior was not observed; rather ζ was seen to be a function of ℓ and R (see Fig. 6). This effective exponent decreased to a very small value when ℓ dropped below approximately 0.3 mm. The approach of ζ to zero (rather than the expected value of unity [8]) at small ℓ has also been seen in grid-generated turbulent flow [9, 10], in turbulent pipe flow at large R, and in Rayleigh-Bénard convection [11]. It is possible that in all these

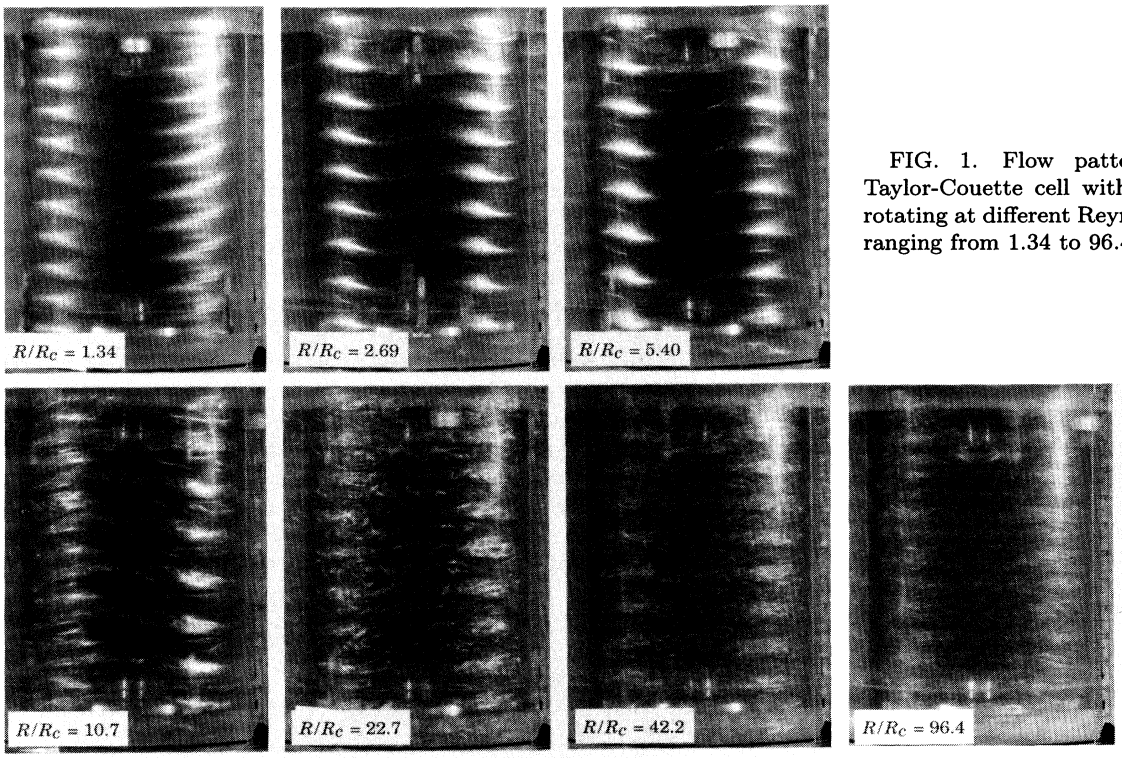

FIG. 1. Flow pattern observed in a Taylor-Couette cell with the inner cylinder rotating at different Reynolds numbers R/R_c ranging from 1.34 to 96.4.

experiments, this effect could be an artifact linked with the finite radius of the laser beam. For reasons to be given below, we believe that it is not an artifact and may be an important new effect.

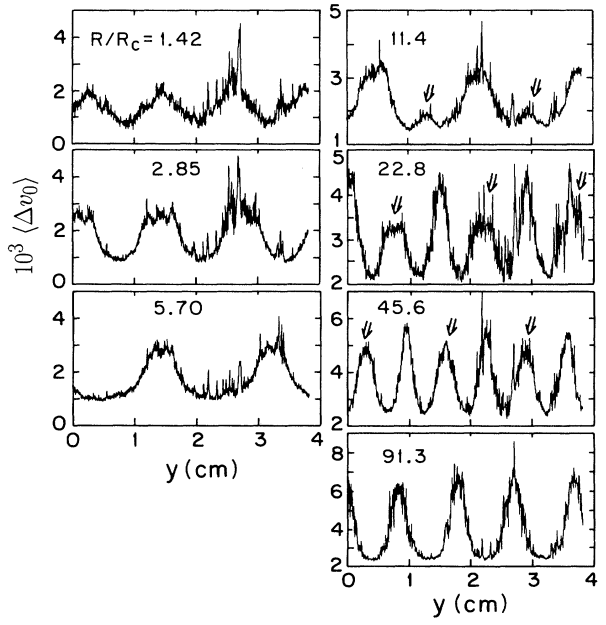

FIG. 2. The dependence of the dimensionless velocity $\langle \Delta v_0(y) \rangle$ as a function of height in a Taylor-Couette cell at different Reynolds numbers R/R_c ranging from 1.42 to 91.3. The arrows indicate the new local maxima which are described in the text.

EXPERIMENTS

Figure 3 shows the experimental arrangement. Only the inner cylinder was rotated with a rotational frequency ω. The gap between the two cylinders was filled with water and now seeded with uniform polestyrene particles of diameter 0.106 μm. The radius of the inner cylinder is $R_1 = 46.88$ mm and the radius of the outer cylinder is $R_2 = 52.45$ mm. A laser beam, traveling in the horizontal direction, is focused with a lens of focal length $f_1 = 10$ cm. The beam waist diameter was 0.10 mm and was located at the center of the gap. (The diameter of the beam is defined as the width where the intensity has decreased by a factor $1/e$ from the intensity at the center of the beam.) Figure 4(a) shows the scattering geom-

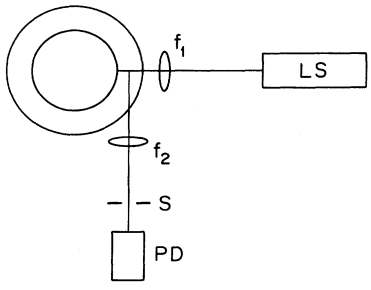

FIG. 3. Experimental arrangement for the HCS Couette flow measurements. The focal lengths of the lenses are $f_1 = 20$ cm and $f_2 = 10$ cm. S is an adjustable slit, PD the photodetector, and LS a He-Ne laser.

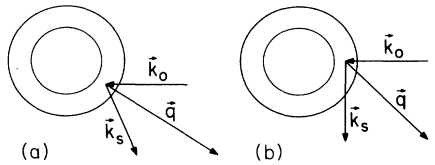

FIG. 4. Top view of flow cells at different scattering geometry. Here $\mathbf{k_0}$ is the incident, $\mathbf{k_s}$ is the scattered wave vector, and $\mathbf{q} = \mathbf{k_s} - \mathbf{k_0}$ the momentum transfer vector. The scattering geometry in (a) was used in the vertical measurements of the correlation function, and geometry (b) was used in the measurements at one fixed position with different slit widths.

etry, which is chosen to probe the velocity components in a "near" radial direction. This geometry was used in the measurements of the velocity fluctuations as a function of height. One reason to choose this geometry is the radial symmetry of the problem. Due to the velocity shear between the inner and the other cylinder, we expect the velocity difference $\langle \delta v(l,y) \rangle$ to be smaller along the radial than the azimuthal direction. This will imply a longer decay time of the correlation function when $\mathbf{q}$ is directed in radial than in azimuthal direction. With our setup the limitation at high Reynolds numbers is the dead time of our photodiode which is about 200 ns.

The scattering geometry in Fig. 4(b) was used for convenience in the measurement of the ℓ dependence of $\langle \delta v(\ell,y) \rangle$ because it is easier to align than the geometry in Fig. 4(a). The aspect ratio of the Couette cell is $\kappa = h/(R_2 - R_1) = 19.9$, and the height h of the inner cylinder is 11.1 cm. The top and bottom of the inner cylinder were not closed off to prevent fluid flow at the ends. The seed particles scatter light, and a lens of focal length $f_2 = 10$ cm is used to form an 1:1 image of the scattering volume, centered onto a slit of adjustable width.

The scattered light falls on a RCA model SPCM-100-PQ photodiode positioned 35 cm from the slit, and the signal from the photodiode is fed into a Malvern correlator, model K7025. All the optics, including the laser, are mounted on a computer-controlled translation stage, which enables movement of the laser beam in the vertical direction with a total displacement of 4 cm. The measurements were started with the laser beam positioned 4.0 cm from the bottom of the inner cylinder and the beam is moved vertically in steps of 0.038 mm between each measurement of the correlation function. A thousand correlation functions [therefore 1000 values of $\langle \delta v(y) \rangle$] are measured in each full vertical scan.

The flow pattern was visually observed, using Kalliroscope particles, at each value of R at which $\langle \delta v(y) \rangle$ was measured. These particles are small platelets that are aligned by the local flow field and reflect light. Because the Kalliroscopic flakes must be removed and replaced with the smaller seed particles needed to measure $\langle \delta v(y) \rangle$, it was not possible to relate visually observed structure with the light scattering measurements. The reason is that specifying R does not uniquely specify the position and the spacing of the rolls [4, 12]. Thus there was no way to determine if the maxima in $\langle \delta v(y) \rangle$ occurred at the vertical positions of outflow or inflow.

LIGHT SCATTERING

In the homodyne correlation spectroscopy technique one measures the intensity correlation function of the scattered light, given by

$$g(\tau) = \left\langle \int_A I(t)dA \int_{A'} I(t+\tau)dA' \right\rangle \Big/ \left\langle \int_A I(t)dA \right\rangle^2 , \tag{1}$$

where the integrations are over the detector area. When light is scattered from a particle moving in a fluid with velocity $\mathbf{v}$, the frequency is Doppler shifted. This shift is $\mathbf{v} \cdot (\mathbf{k_s} - \mathbf{k_0})$, where $\mathbf{k_s}$ and $\mathbf{k_0}$ are the wave vectors of the scattered and the incident light, respectively. The magnitude of $\mathbf{k_0}$ is $k_0 = n2\pi/\lambda$, where n is the index of refraction of the fluid and λ the vacuum wavelength. It turns out that the only important contribution to the correlation function will be from beating terms of all particle pairs [9]. For a detector of circular area $g(\tau)$ becomes [9, 13]

$$g(\tau) = 1 + 4 \int_0^l \int_{\delta v} (2/\ell)(1 - r/\ell) \cos(q\delta v \tau) P(\delta v, r) \left[\frac{J_1(k_0 a r/2R)}{k_0 a r/2R} \right]^2 d\delta v dr , \tag{2}$$

where $P(\delta v, r)$ is the probability that two points in the fluid, separated with a distance r, have a velocity difference δv. Recall that δv is the projection of the velocity difference $\delta \mathbf{v}(l)$ in the direction of the momentum transfer vector $\mathbf{q} = \mathbf{k_0} - \mathbf{k_s}$. The factor, $\cos(q\delta v \tau)$, is the Doppler beating term from particle pairs, and $(2/\ell)(1 - r/\ell)$ [9] is the probability density of particle pairs separated by a distance r within a total length ℓ. Of necessity the photodetector is of finite area, and hence one must integrate over it. This integration introduces the last factor $J_1(x)/x$, where $x = k_0 a r/2R$ in the correlation function. This is a coherence factor, and will decrease with the separation distance of the particle pairs [13]. It is important to note that spatial coherence effects are much more important in these experiments than in the case of pure diffusion, because the shape of the correlation function depends on the size and the shape of the detector. In the case of light scattering by diffusing particles, this spatial averaging reduces the amplitude of the time-dependent part of the intensity correlation function $g(\tau)$, but it does not change its functional form [14].

The decay time of the correlation function $G(\tau) \equiv g(\tau) - 1$ is inversely proportional to the characteristic velocity difference $\langle \delta v(\ell,y) \rangle$ on a length scale l. For the

discussion to follow, it is useful to define two characteristic times: $\tau_0 = \int G(\tau)d\tau$, and $\tau_{1/2}$ which is given by $G(\tau_{1/2}) = 1/2$. It is also convenient to define two characteristic dimensionless velocities, $\langle \Delta v_0(y) \rangle = (q\tau_0 R_1 \omega)^{-1}$ and $\langle \Delta v_{1/2}(y) \rangle = (q\tau_{1/2} R_1 \omega)^{-1}$.

The function $G(\tau)$ is also dependent on the parameters ℓ and R. It follows from Eq. (2) that if $P(\delta v, r)$ has the scaling form, $P(\delta v, r) = \langle \delta v(r,y) \rangle^{-1} Q(\delta v / \langle \delta v(r,y) \rangle)$, and if $\langle \delta v(r,y) \rangle \sim r^\gamma$, then $G(\tau)$ will have the scaling form

$$G(q, \tau, \ell, y) = G(q \langle \delta v(\ell) \rangle \tau, y). \tag{3}$$

It is assumed here that the coherence factor $J_1(x)/x$ in the square brackets of Eq. (2) is constant.

DISCUSSION

Figure 2 shows the measured dimensionless velocities $\langle \Delta v_0(y) \rangle$. These measurements were made with $\ell = 0.2$ mm and at the indicated Reynolds numbers, R/R_c, which range from 1.42 to 91.3. The critical Reynolds number was measured to $R_c = 125 \pm 5$ by visualization experiment. It is important to understand the experimental procedure. Each time the rotation frequency of the inner cylinder was changed, the driving motor was turned off and remained so until the fluid became quiescent. Then the inner cylinder was rapidly accelerated to the desired frequency. Attention is again drawn to the fact that the spatial periodicity of $\langle \Delta v_0(y) \rangle$ is approximately the same as the roll spacing seen in Fig. 1.

The small-scale noise in $\langle \Delta v_0(y) \rangle$, which is of the order of 7% of its value, corresponds to the statistical noise. The large-scale fluctuations which are more frequently at large heights are an artifact due to reflection problems. This noise is independent of the different rotation velocities of the inner cylinder, and appears at the same value of y for all measurements.

The number of azimuthal waves in the cell will depend on the early history of a run. The measurements were repeated many times with no effort made to keep the initial ramp-up rate precisely the same. Yet we almost always saw the same pattern by eye and by homodyne measurement. Moreover, the main results presented in this paper would seem to be independent of the precise state being investigated. Figure 1 shows the observed flow patterns, recorded at approximately the same values of R/R_c as in the HCS measurements of Fig. 2. For $R/R_c = 1.34$ (Fig. 1) the system is in the wavy vortex flow regime, the distance between the azimuthal waves being approximately 1.0 cm. The periodicity of $\langle \Delta v_0(y) \rangle$ is almost the same, even though the two experiments are probing the system on quite different spatial scales. When the rotation frequency is increased further, the periodicity of $\langle \Delta v_0(y) \rangle$ changes, as seen at Reynolds numbers $R/R_c = 2.85$ and $R/R_c = 5.70$ in Fig. 2. Note that the wavelength of the large-scale periodicity increases on increasing the Reynolds number. This increase is also seen in the visualization experiments. At $R/R_c = 5.40$ the periodicity a in Fig. 1 is 1.5 cm, whereas $a = 1.8$ cm in the corresponding HCS measurement with $R/R_c = 5.70$. This is surely the result of the fact that the preparation of the states in these experiments was slightly different, in spite of the fact that R/R_c was approximately the same.

At $R/R_c = 11.4$ new maxima in $\langle \Delta v_0(y) \rangle$ appear at the positions indicated by the arrows in Fig. 2. This new feature occurs at a Reynolds number close to $R/R_c = 10.1$, which is where the transition to modulated wavy vortex flow occurs [12, 3] with a cell similar in construction to ours, but which has closed boundary conditions. (As a check, we also performed experiments in the same cell as the one used here but with closed boundary conditions, and observed a secondary maximum at Reynolds number R/R_c =11.0.) On the other hand, the transition displayed in Fig. 2 also occurs at a value of R/R_c which is close to R/R_c=12, the dimensionless Reynolds number at which broadband chaotic fluctuations first appear [3, 4]. The amplitude of these new maxima becomes equal to the amplitude of the primary maxima in $\langle \Delta v_0(y) \rangle$ as R increases. A closer inspection of the flow visualization experiment in Fig. 1 also shows small-scale spatial fluctuations at $R/R_c = 10.7$. At $R/R_c = 91.3$ (Fig. 5), primary and secondary maxima are seen to become indistinguishable. This small-scale periodicity persists deep into the turbulent regime, where the wavy vortex fluctuations have vanished. The modulated wavy vortex flow is well known to disappear at Reynolds numbers above about 19, but the chaotic broadband component will be present at all higher Reynolds numbers. Our new maxima *do not* disappear at Reynolds number higher than 19 but are present deep into the turbulent vortex flow regime. This implies that the new maxima are not correlated with the modulated wavy vortex flow. These experiments suggest to us that the amplitude of the broadband component of the power spectrum $S(\omega)$ of the local velocity field $v(t)$, measured by others [3, 4], will vary periodically with y. Presently we have no measurements to support this speculation.

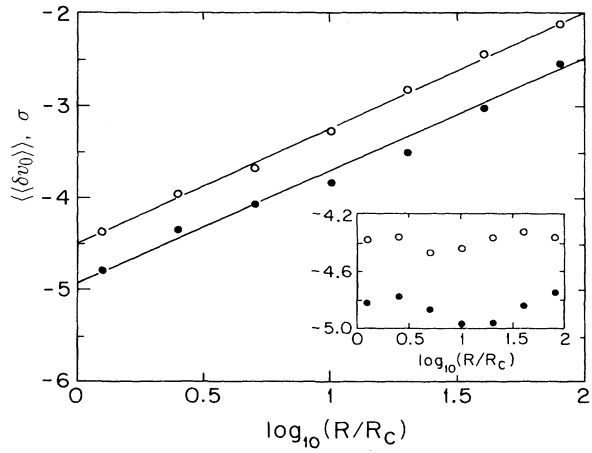

FIG. 5. Open circles: The dependence of the average velocity $\langle\langle \delta v_0 \rangle\rangle$ on the Reynolds number in a Taylor-Couette cell. Closed circles: The dependence of the standard deviation σ on the Reynolds number. Solid lines have slopes of 1.25. The inset shows $\log_{10}\left[\langle\langle \delta v_0 \rangle\rangle/(R/R_c)^{1.25}\right]$ as a function of $\log_{10} R/R_c$ (open circles), and $\log_{10}\left[\sigma/(R/R_c)^{1.25}\right]$ as a function of $\log_{10} R/R_c$ (closed circles).

Though the large-scale structure of the flow is not uniquely determined by R, we nonetheless have found that the y average of $\langle \delta v_0(y) \rangle$ (which we write as $\langle\langle \delta v_0 \rangle\rangle$) is smoothly dependent on the Reynolds number, i.e., on the mean flow velocity $U = R_1\Omega$. This is seen in Fig. 5 (open circles), which is a double logrithmic plot of $\langle\langle \delta v_0 \rangle\rangle$, as well as its standard deviation, as a function versus R. The latter quantity is designated as σ and is shown in Fig. 5 (closed circles). Similar curves were obtained when the average velocity $\langle\langle \delta v_0 \rangle\rangle$ was replaced by $\langle\langle \delta v_{1/2} \rangle\rangle$. As a guide for the eye we have also shown in the figure lines of slope $\alpha = 1.25$. This slope is the average slope obtained by fitting all the data points to a linear curve, and was obtained for both $\langle\langle \delta v_0 \rangle\rangle$ and σ. However, the data points show clear oscillations in $\langle\langle \delta v_0 \rangle\rangle$ and σ around the curve of slope $\alpha = 1.25$, as seen in the inset of Fig. 5. This indicates lack of scaling, and suggests that the exponent α is not well defined and must be considered as an average exponent, $\alpha = \beta = 1.25 \pm 0.07$.

It is interesting to compare the above observations $\langle\langle \delta v_0 \rangle\rangle \sim R^{1.25}$ with expectations based on the Kolmogorov theory in one limit, and on the assumption of laminar flow in the other. The result in both cases is

$$\langle \delta v(\ell) \rangle \simeq (\ell/\ell_0)^\gamma \langle \delta v(\ell_0) \rangle = (\ell/\ell_0)^\gamma R\nu/\ell_0 \,, \qquad (4)$$

with γ =1 in the laminar case and 1/3 in the Kolmogorov model. Because the flow is very far from being isotropic or homogeneous in our Couette cell, one hardly expects Kolmogorov theory to apply. Nevertheless, in other experiments using a Couette cell of much smaller aspect ratio than that used here, the exponent γ was measured to be close to 1/3 at large R [7].

Our determination of the dependence of $\langle\langle \delta v_0 \rangle\rangle$ on R is a robust one in the sense that it was extracted from the measurement of thousands of correlation functions (measured at various values of y). The data are clearly inconsistent with $\alpha = 1.0$, and show lack of scaling with an effective exponent oscillating around $\alpha = 1.25$.

Next, consider how the measured values of $\langle \delta v(\ell, y) \rangle$ vary with ℓ at a fixed value of $y = 5$ cm. Here the simplified notation $\langle \delta v(\ell, y = 5 \text{ cm}) \rangle \equiv \langle \delta v(\ell) \rangle$ is used. The goal here is to see if the measurements are consistent with Eq. (4). Figure 6 is a $\log_{10}$-$\log_{10}$ plot of $\langle\langle \delta v_0(\ell) \rangle\rangle$ as a function of the normalized slit width, ℓ for several values of R/R_c, namely 10.2 (closed circles), 20.5 (crosses), and 52.0 (open circles). The data points do not lie on lines of constant slope and are therefore inconsistent with Eq. (4). Because of spatial coherence effects [13], the measurements in that figure are most trustworthy at the smaller values of ℓ. The measurements at the two lowest values of R are in a regime where a numerical analysis of the Navier-Stokes equation for Couette flow has been carried out [15].

The failure of the scaling law, $\langle \delta v_0(\ell) \rangle \sim \ell^\gamma$ can also be seen in the fact that $g(\tau)$ does not have the scaling form given by Eq. (3). Were this scaling to obtain, a plot of $G(q\tau\ell^\gamma)$ would yield a single curve for all values of ℓ. Figure 7 is such a plot on a $\log_{10}$-$\log_{10}$ scale. The curves shown here correspond to ℓ ranging from 0.2 mm to 1.89 mm. The self-similarity of the curves was "best" when γ was selected to be 0.7. The measurements shown

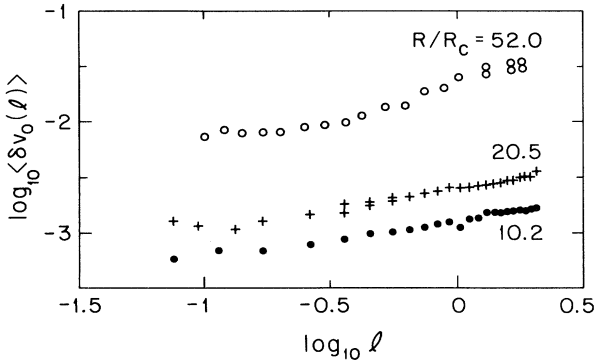

FIG. 6. Characteristic velocity $\langle \delta v_0(\ell) \rangle$ as function of slit width l at the indicated Reynolds numbers R/R_c.

here were also made at a height y in the approximate middle of the cell. For these data, R/R_c was 51.9. The absence of scaling is self-evident. It appears from Fig. 6 that γ is approaching zero as ℓ decreases, a result that is also seen in studies of grid-generated and pipe-generated turbulent flow [9, 10] and in a study of the velocity field in Rayleigh-Bénard convection [11]. It is not surprising that Taylor-Couette flow at $R/R_c < 100$ is not turbulent in the Kolmogorov sense. What is surprising, however, is that the curve becomes flat at small length scales. This interesting finding is inconsistent with all existing theories of turbulence which predict a linear dependence on small length scales [8]. The observed ℓ independence of $\langle \delta v_0(\ell) \rangle$ suggests that there is in the flow a characteristic length scale η that is smaller than the minimum value of ℓ which was attainable in these experiments. We have no way of measuring η, and hence no way of determining if this length scale is correctly identified with the dissipative length scale appearing in the Kolmogorov theory.

It is important to be sure that the flattening of $\langle \delta v_0(\ell) \rangle$ at small length scales is not an experimental artifact arising from the finite beam diameter d. If d is larger than the slit width ℓ, measured velocity differences will be governed by this length rather than ℓ, and $\langle \delta v_0(\ell) \rangle$ will obviously become independent of ℓ. To determine if the flattening of the curves at small ℓ in Fig. 6 was due to

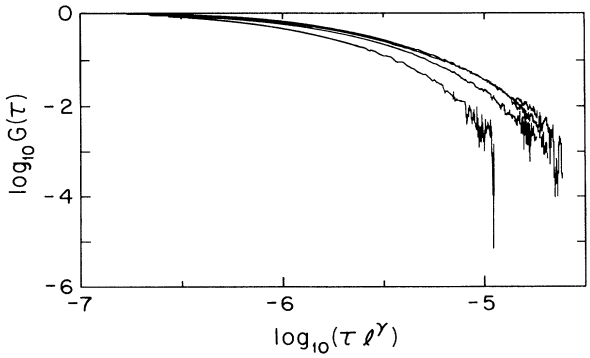

FIG. 7. The correlation function $G(\tau)$ as function of $\tau l^{0.7}$ for different slit widths 0.1, 0.2, 0.42, 0.89, and 1.89 mm. The Reynolds number is $R/R_c = 51.9$.

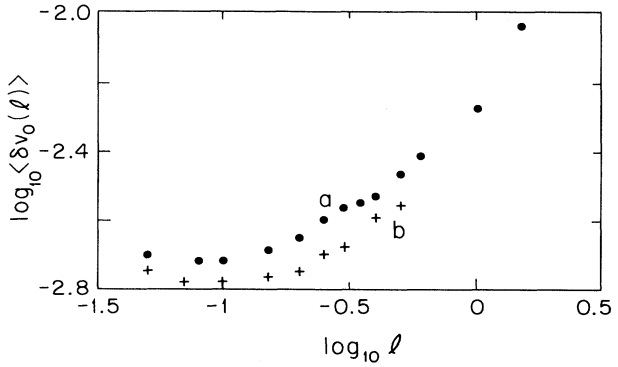

FIG. 8. The dependence of $\langle \delta v_0(l) \rangle$ on slit width l. Curve a: Expanded beam-beam diameter $d = 0.3$ mm. Curve b: Focused beam of diameter $d = 0.05$ mm. Reynolds number $R/R_c = 23.1$.

the finite diameter of the laser beam, we deliberately increased d, by a factor 5, to see if the flattening appeared at a smaller value of ℓ. The results appear in Fig. 8, which is a plot of $\log_{10}\langle \delta V_0(\ell) \rangle$ vs $\log_{10}\ell$, with ℓ in mm. For curve a, $d = 0.3$ mm; for curve b, $d = 0.05$ mm. Here $y = 5$ cm and $R/R_c = 23.1$, which is in the turbulent-vortex-flow regime. The vertical shift between the two curves is due to a small difference in the scattering angle between curves a and b. The knee in the curves appears at approximately the same value of ℓ for both curves, suggesting that the small slope at small ℓ is not an optical artifact.

CONCLUSION

Homodyne correlation spectroscopy has been used to measure spatial inhomogeneities $\langle \delta v(y, l) \rangle$ in a Taylor-Couette cell, on length scales ℓ much smaller than the gap width. These measurements have been performed for R/R_c ranging from 1.4 to 91. Even at the highest achievable values of R, $\langle \delta v(\ell = 0.2 \text{ mm}, y) \rangle$ oscillates as a function of vertical position in the cell. These oscillations are highly correlated with the large-scale fluctuations observed by visualization techniques. A new local maximum in the small-scale fluctuations appears at a Reynolds number close to the onset of chaos. The amplitude of this spatial inhomogeneity increases with increasing R far into the turbulent vortex regime.

The height-averaged value $\langle\langle \delta v(y) \rangle\rangle$ and its standard deviation show lack of scaling, but has an average exponent α equal to 1.25. It was not surprising that $\langle\langle \delta v_0 \rangle\rangle$ fails to scale as a power of R, since the visualization measurements reveal spatial inhomogeniety even at the highest values of R/R_c.

We also observed a failure of the scaling law $\langle \delta v_0 \rangle \sim l^{\gamma}$. At small ℓ, $\langle \delta v(\ell, y = 5 \text{ cm}) \rangle$ becomes independent of ℓ, a result that has appeared in homodyne correlation studies of strongly turbulent flows and Rayleigh-Bénard convection studies at very high Rayleigh numbers. The observed independence of $\langle \delta v(\ell) \rangle$ suggests the existence of a small length scale in the flow which is smaller than the minimum length scale attainable in this experiment.

ACKNOWLEDGMENTS

We thank Xiao Lun Wu for stimulating discussions. This work has been supported by the National Science Foundation, Grant No. DMR-8914351. K.J.M. was also supported by the Norwegian Council for Science and Humanities (NAVF).

* Present address: Fysisk Institutt, Universitetet i Oslo, N-0316 Oslo 3, Norway.

[1] H. L. Swinney and J. P. Gollub, *Hydrodynamic Instabilities and the Transition to Turbulence*, 2nd ed. (Springer-Verlag, New York, 1985).
[2] E. L. Koschmider, J. Fluid Mech. **93**, 515 (1979).
[3] J. P. Gollub and H. L. Swinney, Phys. Rev. Lett. **35**, 927 (1975).
[4] P. R. Fenstermacher, H. L. Swinney, and J. P. Gollub, J. Fluid. Mech. **94**, 103 (1979).
[5] A. N. Kolmogorov, Dokl. Akad. Nauk SSSR **30**, 301 (1941); for English translation, see Proc. R. Soc. London Ser. A **434**, 9 (1991).
[6] H. Tennekes, *A First Course in Turbulence* (MIT Press, Cambridge, MA, 1972).
[7] P. Tong, W. I. Goldburg, and J. S. Huang, Phys Rev. A **45**, 7231 (1992).
[8] L. Landau and E. M. Lifshitz, *Fluid Mechanics* (Pergamon, New York, 1987).
[9] P. Tong, W. I. Goldburg, C. K. Chan, and A. Sirivat, Phys. Rev. A **37**, 2125 (1988).
[10] H. K. Pak, W. I. Goldburg, and A. Sirivat, Fluid Dynamics Research, **8**, 19 (1991).
[11] P. Tong and Y. Shen, Phys. Rev. Lett. **69**, 2066 (1992).
[12] M. Gorman and H. L. Swinney, J. Fluid Mech. **117**, 123 (1982).
[13] K. J. Måløy, W. I. Goldburg, and H. K. Pak, Phys. Rev. A **46**, 3288 (1992).
[14] E. Jakeman, C. J. Oliver, and E. R. Pike, J. Phys. A **3**, L45 (1970).
[15] P. S. Marcus, J. Fluid Mech. **146**, 45 (1984); **146**, 65 (1984).

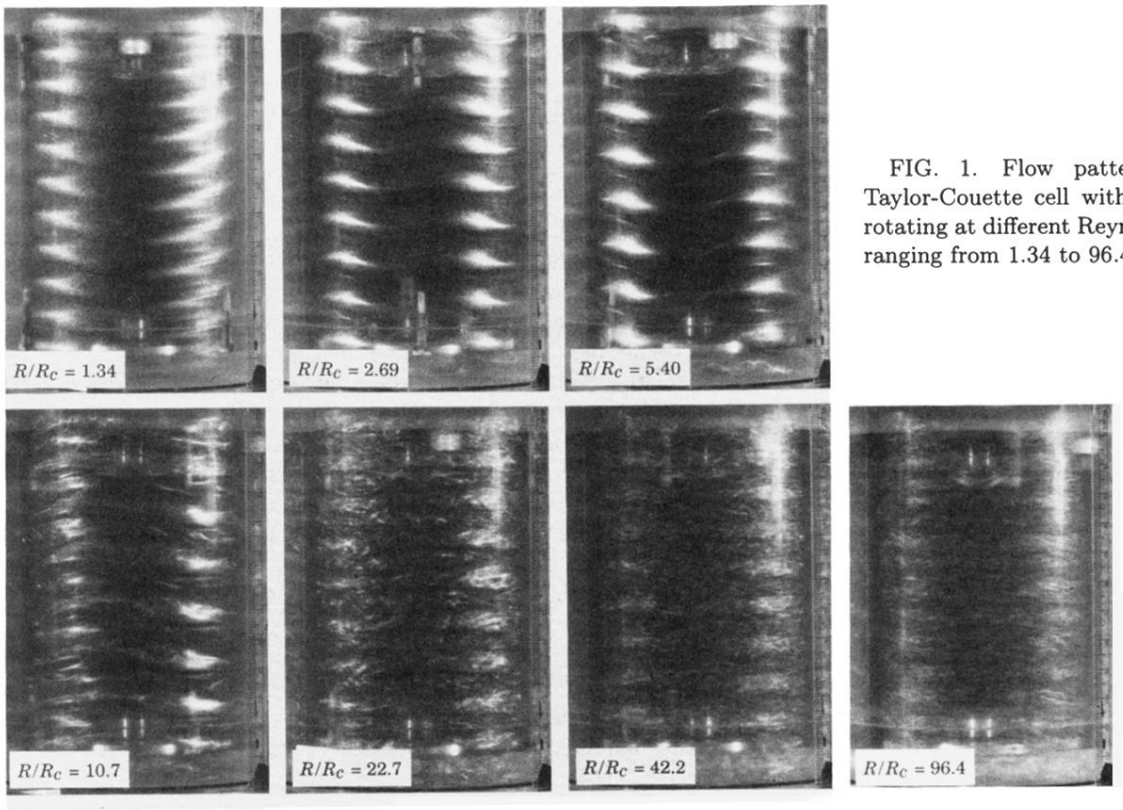

FIG. 1. Flow pattern observed in a Taylor-Couette cell with the inner cylinder rotating at different Reynolds numbers R/R_c ranging from 1.34 to 96.4.